A simple mass-action model for the eukaryotic heat shock response and its mathematical validation

Ion Petre[1,*], Andrzej Mizera[1], Claire L. Hyder[2,3], Annika Meinander[2,3], Andrey Mikhailov[2,3], Richard I. Morimoto[4], Lea Sistonen[2,3], John E. Eriksson[2,3], Ralph-Johan Back[1]

[1] Department of IT, Åbo Akademi University
Turku 20520, Finland
[2] Turku Centre for Biotechnology
[3] Department of Biosciences, Åbo Akademi University
Turku 20520, Finland
[4] Department of Biochemistry, Molecular Biology and Cell Biology,
Rice Institute for Biomedical Research,
Northwestern University, Evanston, Illinois 60208
∗ Corresponding author. Email: ipetre@abo.fi

Abstract

The heat shock response is a primordial defense mechanism against cell stress and protein misfolding. It proceeds with the minimum number of mechanisms that any regulatory network must include, a stress-induced activation and a feedback regulation, and can thus be regarded as the archetype for a cellular regulatory process. We propose here a simple mechanistic model for the eukaryotic heat shock response, including its mathematical validation. Based on numerical predictions of the model and on its sensitivity analysis, we minimize the model by identifying the reactions with marginal contribution to the heat shock response. As the heat shock response is a very basic and conserved regulatory network, our analysis of the network provides a useful foundation for modeling strategies of more complex cellular processes.

Keywords: Heat shock response; heat shock protein; heat shock factor; heat shock element; mathematical model; validation; regulatory network.

Introduction

The heat shock response is an ancient, evolutionary conserved regulatory mechanism that allows the cell to quickly react to elevated temperatures and other

forms of physiological and environmental stress. The heat shock response has been subject of active research, see [1–3], for at least two reasons. On one hand, as it represents an exceptionally well-conserved signaling mechanism, it is a good candidate for deciphering the mechanistic principles of gene regulatory networks. On the other hand, heat shock proteins have essential roles in all aspects of protein biogenesis, regardless of the regulatory aspects of the heat shock response, and have fundamental importance for many key biological processes. Therefore, understanding the details of the heat shock response has broad ramifications for the the biology of the cell and response to cellular insults and for the onset and treatment of a number of diseases, including neurodegenerative disorders, cancer, aging, and cardiovascular diseases, see [4, 5].

Despite intense research and a number of models that have been presented to cover the heat shock response, a comprehensive mechanistic understanding of this process is lacking. Here, we propose a simple model capturing in mechanistic details all key aspects of the regulation: the heat-induced protein misfolding, the chaperone activity of heat shock proteins, the transactivation of the genes encoding heat shock proteins and the repression of their transcription once the stress is removed. In contrast with previous attempts to model the eukaryotic heat shock response, our model is based solely on well-documented molecular reactions and does not include modeling "blackboxes" such as experimentally unsupported components and biochemical reactions.

We also present a mathematical model associated with the model and its experimental validation. For specific parameter estimation and model validation, we use already published data [6], as well as new experimental data. The model predictions correlate well with experimental data on the heat-induced transactivation of the genes encoding heat shock proteins at various temperatures, its return to the original level once the stress is removed, and a lower response to a second consecutive heat shock. We use the model to identify a number of reactions that could be eliminated from the model without affecting its quantitative behavior. We also identify the most significant reactions regulating the levels of the heat shock proteins and those of the misfolded proteins. This analysis deepens our understanding of where the significant control resides in the network.

Results

Molecular model The heat shock protein (hsp) plays the central role as a chaperone to prevent misfolding, to capture intermediates, and to facilitate protein folding. Even though there are multiple classes of hsps, with various molecular masses and different regulatory mechanisms, we treated them all uniformly in our model, with hsp 70 as the base denominator. The hsp-encoding genes are transactivated through the binding of heat shock factors (hsf) to the heat shock element (hse) found on the DNA upstream of the gene. Even though several types of heat shock factors exist (HSFs1-4), see [7], we focused on HSF1 in our model. The binding of a heat shock factor trimer (hsf_3) to a heat shock element was denoted as hsf_3: hse. Heat shock proteins may bind to heat shock factors; we denoted such a bond as hsp: hsf. The drivers of the whole heat shock response are the heat-induced misfolded proteins, denoted mfp. Binding of a heat shock protein to a misfolded protein was denoted as hsp: mfp. We made no

distinction among the many types of protein substrates that exist in the cell. From the point of view of the heat shock response, we were only interested in whether they are correctly folded (collected globally under the name prot), or misfolded (collected globally under the name mfp). What drives the heat shock response is the race to keep the level of misfolded proteins under control, in such a way that they are not able to accumulate, form aggregates, and eventually lead to cell death.

Our molecular model for the heat shock response consists of three parts: the dynamic transactivation of the hsp-encoding genes, their backregulation, and the chaperone activity of the hsp. In the absence of the heat stress, the heat shock factors are present as monomers, mainly bounded to heat shock proteins. There is insignificant variation in their concentration with stress. Upon heat stress however, the heat shock factors form trimers, which are the active components, able to bind to heat shock elements, see [8, 9]. Once hsf_3 is bound to the heat shock element, we assumed that the hsp-encoding gene is transcriptionally active. We did not model explicitly the transcription machinery binding to the promoter region of the hsp-encoding gene, the mRNA molecules being produced, edited, transported, etc., but only represented that a transcriptionally active hsp-encoding gene will eventually yield the synthesis of new hsp molecules, see reaction (4) in Table 1. Heat shock proteins have an affinity for heat shock factors and so, if present in sufficient amounts, are able to shut down their own synthesis: a heat shock protein hsp contributes to unbinding a trimer hsf_3 from the heat shock element, see reaction (8) in Table 1 and [10, 11].

Table 1: **The list of reactions in the molecular model for the heat shock response.**

Reaction	(Reaction number)
$2\,\mathsf{hsf} \leftrightarrow \mathsf{hsf}_2$	(1)
$\mathsf{hsf} + \mathsf{hsf}_2 \leftrightarrow \mathsf{hsf}_3$	(2)
$\mathsf{hsf}_3 + \mathsf{hse} \leftrightarrow \mathsf{hsf}_3\colon \mathsf{hse}$	(3)
$\mathsf{hsf}_3\colon \mathsf{hse} \rightarrow \mathsf{hsf}_3\colon \mathsf{hse} + \mathsf{hsp}$	(4)
$\mathsf{hsp} + \mathsf{hsf} \leftrightarrow \mathsf{hsp}\colon \mathsf{hsf}$	(5)
$\mathsf{hsp} + \mathsf{hsf}_2 \rightarrow \mathsf{hsp}\colon \mathsf{hsf} + \mathsf{hsf}$	(6)
$\mathsf{hsp} + \mathsf{hsf}_3 \rightarrow \mathsf{hsp}\colon \mathsf{hsf} + 2\,\mathsf{hsf}$	(7)
$\mathsf{hsp} + \mathsf{hsf}_3\colon \mathsf{hse} \rightarrow \mathsf{hsp}\colon \mathsf{hsf} + \mathsf{hse} + 2\,\mathsf{hsf}$	(8)
$\mathsf{hsp} \rightarrow$	(9)
$\mathsf{prot} \rightarrow \mathsf{mfp}$	(10)
$\mathsf{hsp} + \mathsf{mfp} \leftrightarrow \mathsf{hsp}\colon \mathsf{mfp}$	(11)
$\mathsf{hsp}\colon \mathsf{mfp} \rightarrow \mathsf{hsp} + \mathsf{prot}$	(12)

The heat-induced misfolding of proteins was represented in our model as a reaction switching an unfolded or native protein (prot) to misfolded (mfp). The reaction rate depends exponentially on the temperature of the environment,

see [12, 13]. A heat shock protein may chaperone a misfolded protein and facilitate its refolding. The list of all reactions in our molecular model is given in Table 1.

There are three conservation relations in our model. One concerns the total amount of hsf:

$$[\mathsf{hsf}] + 2 \times [\mathsf{hsf}_2] + 3 \times [\mathsf{hsf}_3] + 3 \times [\mathsf{hsf}_3\colon \mathsf{hse}] + [\mathsf{hsp}\colon \mathsf{hsf}] = \text{constant}. \quad \text{(C1)}$$

The second concerns the total amount of proteins, other than hsp and hsf:

$$[\mathsf{prot}] + [\mathsf{mfp}] + [\mathsf{hsp}\colon \mathsf{mfp}] = \text{constant}. \quad \text{(C2)}$$

The third concerns the total amount of heat shock elements:

$$[\mathsf{hse}] + [\mathsf{hsf}_3\colon \mathsf{hse}] = \text{constant}. \quad \text{(C3)}$$

The only variable of the model not covered by the conservation relations is hsp, which is the regulatory target of the heat shock response.

Mathematical model and parameter estimation In developing the mathematical model, we assumed for all reactions the principle of *mass-action*, that can be briefly summarized as follows: the flux of each reaction is proportional to the amount of input to the reaction, see [14], [15]. The reason why we preferred a simple mass-action formalization rather than more sophisticated approaches such as Michaelis-Menten or Hill equations was so that we could follow the explicit effect of each individual reaction to the overall response. We expressed our model in terms of differential equations, with one function associated to each component in the model. The resulting mathematical model consists of ten differential equations and is shown in Table 2. Of these ten equations, based on the conservation relations (C1)-(C3), only seven equations are independent. In Table 2, we denoted by k_i the reaction rate constant of the irreversible reaction (i) in Table 1, by k_i^+, the reaction rate constant corresponding to the 'left-to-right' direction of the reversible reaction (i) in the same table, while k_i^- denotes the rate constant corresponding to its 'right-to-left' direction, for all $1 \leq i \leq 12$. We denoted by T the temperature of the environment.

The extent of heat-induced protein denaturation in CHL V79 cells has been investigated in [13]. Based on that study, the fractional protein denaturation per hour was deduced in [12]. Since our model uses the second as time unit, we adapted the fractional protein denaturation per second ϕ_T from [12] to obtain the temperature-dependant formula

$$\phi_T = \left(1 - \frac{0.4}{e^{T-37}}\right) \cdot 1.4^{T-37} \cdot 1.45 \cdot 10^{-5} \quad s^{-1},$$

where T is the temperature of the environment in Celsius degrees. According to [13], this formula is valid for temperatures between $37°C$ and $45°C$.

There are 17 independent parameters in our model and 10 initial conditions that must be specified or estimated. We had on the other hand the three conservation relations (C1)-(C3) that leave only seven initial conditions to specify. In estimating our parameters we used experimental data of [6] on the rate of $\mathsf{hsf}_3\colon \mathsf{hse}$ during a heat shock of HeLa cells at $42°C$. In addition, we also imposed the condition that with the same initial values and the same numerical

Table 2: **The differential equations of the associated mathematical model.**

Equation	(Equation number)
$d[\mathsf{hsf}]/dt = -2k_1^+[\mathsf{hsf}]^2 + 2k_1^-[\mathsf{hsf}_2] - k_2^+[\mathsf{hsf}][\mathsf{hsf}_2] + k_2^-[\mathsf{hsf}_3]$ $- k_5^+[\mathsf{hsf}][\mathsf{hsp}] + k_5^-[\mathsf{hsp{:}\ hsf}] + k_6[\mathsf{hsf}_2][\mathsf{hsp}]$ $+ 2k_7[\mathsf{hsf}_3][\mathsf{hsp}] + 2k_8(\mathsf{hsf_3{:}\ hse})\,\mathsf{hsp}$	(13)
$d[\mathsf{hsf}_2]/dt = k_1^+[\mathsf{hsf}]^2 - k_1^-[\mathsf{hsf}_2] - k_2^+[\mathsf{hsf}][\mathsf{hsf}_2] + k_2^-[\mathsf{hsf}_3]$ $- k_6[\mathsf{hsf}_2][\mathsf{hsp}]$	(14)
$d[\mathsf{hsf}_3]/dt = k_2^+[\mathsf{hsf}][\mathsf{hsf}_2] - k_2^-[\mathsf{hsf}_3] - k_3^+[\mathsf{hsf}_3][\mathsf{hse}] + k_3^-[\mathsf{hsf_3{:}\ hse}]$	(15)
$- k_7[\mathsf{hsf}_3][\mathsf{hsp}]$	(16)
$d[\mathsf{hse}]/dt = -k_3^+[\mathsf{hsf}_3][\mathsf{hse}] + k_3^-[\mathsf{hsf_3{:}\ hse}] + k_8[\mathsf{hsf_3{:}\ hse}][\mathsf{hsp}]$	(17)
$d[\mathsf{hsf_3{:}\ hse}]/dt = k_3^+[\mathsf{hsf}_3][\mathsf{hse}] - k_3^-[\mathsf{hsf_3{:}\ hse}] - k_8[\mathsf{hsf_3{:}\ hse}][\mathsf{hsp}]$	(18)
$d[\mathsf{hsp}]/dt = k_4[\mathsf{hsf_3{:}\ hse}] - k_5^+[\mathsf{hsf}][\mathsf{hsp}] + k_5^-[\mathsf{hsp{:}\ hsf}] - k_6[\mathsf{hsf}_2][\mathsf{hsp}]$ $- k_7[\mathsf{hsf}_3][\mathsf{hsp}] - k_8[\mathsf{hsf_3{:}\ hse}][\mathsf{hsp}] - k_{11}^+[\mathsf{hsp}][\mathsf{mfp}]$ $+ (k_{11}^- + k_{12})[\mathsf{hsp{:}\ mfp}] - k_9[\mathsf{hsp}]$	(19)
$d[\mathsf{hsp{:}\ hsf}]/dt = k_5^+[\mathsf{hsf}][\mathsf{hsp}] - k_5^-[\mathsf{hsp{:}\ hsf}] + k_6[\mathsf{hsf}_2][\mathsf{hsp}]$ $+ k_7[\mathsf{hsf}_3][\mathsf{hsp}] + k_8[\mathsf{hsf_3{:}\ hse}][\mathsf{hsp}]$	(20)
$d[\mathsf{mfp}]/dt = \phi_T[\mathsf{prot}] - k_{11}^+[\mathsf{hsp}][\mathsf{mfp}] + k_{11}^-[\mathsf{hsp{:}\ mfp}]$	(21)
$d[\mathsf{hsp{:}\ mfp}]/dt = k_{11}^+[\mathsf{hsp}][\mathsf{mfp}] - (k_{11}^- + k_{12})[\mathsf{hsp{:}\ mfp}]$	(22)
$d[\mathsf{prot}]/dt = -\phi_T[\mathsf{prot}] + k_{12}[\mathsf{hsp{:}\ mfp}]$	(23)

parameters, the model is at steady state if the temperature is $37°C$ (by definition, the heat shock response is triggered for temperatures upwards of $37°C$). This yields 7 independent algebraic relations on the set of parameters and initial values. Thus, we have altogether 17 independent values that we need to estimate.

By performing parameter estimation in COPASI [16], we obtained the values shown in Table 3 that satisfy the conditions above. The model fit with respect to the data in [6] is shown in Figure 1A.

Model validation In the final model, we obtained that protein misfolding occurs at $37°C$ at very low rate, that hsp are long-lived molecules, and that the protein folding is a fast reaction, which is in accordance with [17, 18]. (We are disregarding in the model folding intermediates.) Moreover, the model correctly predicted, see [7], that under heat shock, the level of hsf trimers is transiently increased. The model was also able to confirm that the hsf dimers are only a transient state between monomers and trimers and that their level remains low at all times, independent of the temperature.

In another validation test, we considered a heat shock applied in two stages,

Table 3: **The numerical values of the parameters and the initial valus of the variables of the heat shock response model.**

A

Param.	Value	Units
k_1^+	3.49	$\frac{ml}{\#\cdot s}$
k_1^-	0.19	s^{-1}
k_2^+	1.07	$\frac{ml}{\#\cdot s}$
k_2^-	10^{-9}	s^{-1}
k_3^+	0.17	$\frac{ml}{\#\cdot s}$
k_3^-	$1.21 \cdot 10^{-6}$	s^{-1}
k_4	$8.3 \cdot 10^{-3}$	s^{-1}
k_5^+	9.74	$\frac{ml}{\#\cdot s}$
k_5^-	3.56	s^{-1}
k_6	2.33	$\frac{ml}{\#\cdot s}$
k_7	$4.31 \cdot 10^{-5}$	$\frac{ml}{\#\cdot s}$
k_8	$2.73 \cdot 10^{-7}$	$\frac{ml}{\#\cdot s}$
k_9	$3.2 \cdot 10^{-5}$	s^{-1}
k_{11}^+	$3.32 \cdot 10^{-3}$	$\frac{ml}{\#\cdot s}$
k_{11}^-	4.44	s^{-1}
k_{12}	13.94	s^{-1}

B

Variable	Initial conc.
[hsf]	0.67
[hsf_2]	$8.7 \cdot 10^{-4}$
[hsf_3]	$1.2 \cdot 10^{-4}$
[hse]	29.73
[hsf_3: hse]	2.96
[hsp]	766.88
[hsp: hsf]	1403.13
[mfp]	517.352
[hsp: mfp]	71.65
[prot]	1.15×10^8

A. The numerical values of the parameters. B. The initial values of all variables.

with a recovery period between them, with the second shock applied after the level of hsp has reached a maximum. We observed, similarly as in [12], that the predicted response of the model to the second heat shock is much milder, see Figure 2A. This is consistent with the expectation that due to the first heat shock, the level of hsp is already raised, and so the cell may react to the second shock, with a lower [hsf_3: hse] peak.

We also considered a heat shock at $43°C$ and compared our prediction to that of [25]. Similarly as shown by the experimental data in [30], our model was able to show prolonged transactivation, see Figure 2B, unlike the model in [25]. An experiment where the heat shock at $42°C$ is removed at the peak of the response showed a faster attenuation phase, similarly as reported in [25], see Figure 2B. Several sensitivity analysis experiments, where some parameters are set to lower or higher values agreed with the predictions made in similar experiments by [25].

For further verification of our model and its prediction abilities, we performed a set of experiments. Specifically, we aimed to validate the numerical prediction on the level of hsp over time. Our approach was to use a suitable quantitative reporter system based on yellow fluorescent proteins (yfp). Our setup was designed so that the kinetics of the reporter gene's transactivation mimics the results obtained in experimental studies on endogenous hsf target genes. In this way, the dynamics of yfp partially reports on the dynamics of

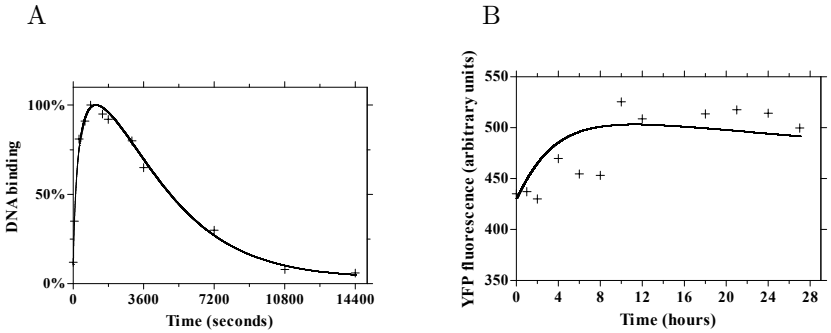

Figure 1: **Comparison of the numerical predictions of the model with two sets of experimental data.** A. The model fit with respect to the experimental data in [6]. The thick line is the model prediction regarding [$\mathsf{hsf_3}$: hse], that is compared with the experimental data showed with crossed points. Both plots are relative to their maximum value. B. Model validation based on fluorescence intensity of cells transfected by hse-controlled genes coding for yellow fluorescent proteins. The crossed dots are the mean values of the experimental data, while the continuous line is the numerical integration of the benchmark variable.

hsp. We did not make any assumptions on the stability of the yfp proteins. Rather, this issue was dealt with in the mathematical validation process. To this aim, we employed K562 cells, expressing a 712 bp fragment of the hsp70 promoter fused to a yellow fluorescent protein (yfp) reporter gene. The cells were subjected to a continuous heat shock at 42°C and samples were taken at indicated time points (for details, see Materials and methods). hsp70 promoter activity as a result of expression of yfp was analyzed by flow cytometry to give a measure of the heat shock response in individual cells.

In three independent biological repeats, we measured the fluorescence intensity of 10000 cells for each time point (15 of them up to 36 hours). Our assumption was that the fluorescence intensity is roughly linear with respect to the level of the yellow fluorescent proteins (yfp) in our sample. Given that the transactivation of the yfp genes is controlled by their own heat shock elements hse′, transcription/translation and degradation kinetics k'_4 and k'_9, resp., we obtained that

$$d[\mathsf{yfp}]/dt = k'_4[\mathsf{hsf_3}\colon \mathsf{hse}'] - k'_9[\mathsf{yfp}],$$

for some positive constants k'_4, k'_9 standing for the kinetic rate constants of the yfp synthesis and of the yfp degradation, respectively. The numerical values of parameters were not deduced from the basic model to underline that we made no assumptions on the stability of yfp, or on their gene transcription rates. The idea of the validation was to extend the already fit basic model so as to include also yfp. In the extended model we re-used all the kinetic rate constants of the basic model. We then looked for numerical values for parameters k'_4 and k'_9 and for initial values of all variables of the model so that the numerical prediction for yfp fit well with the experimental data. The result of the validation is shown in Figure 1B, where the crossed points represent the mean values of the

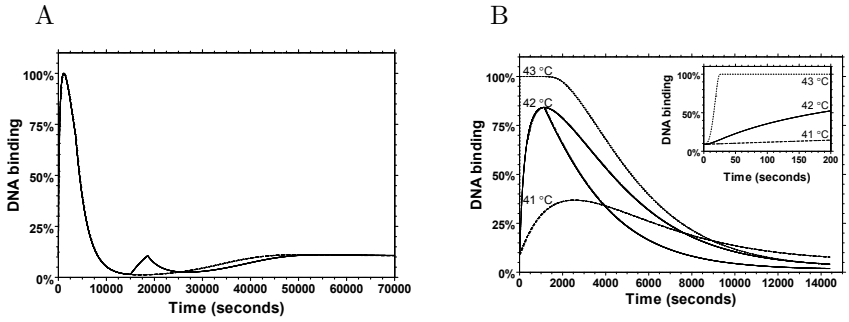

Figure 2: **Numerical predictions of the model.** A. The model correctly predicts that DNA binding peaks at a much lower level in a second consecutive heat shock. The experiment with a single heat shock is shown with a dashed line. B. The model correctly predicts longer transactivation with higher heat shock: the behaviors at $41°C$, $42°C$, and $43°C$ are shown. We also plot on the same graph the correct prediction that the DNA binding attenuates more rapidly in an experiment where the heat shock at $42°C$ is removed at the peak of the response.

experimental data at each time point and the continuous line is the numerical integration of yfp.

Model analysis We estimated the scaled steady state sensitivity coefficients, see [32], of all variables of the model with respect to reaction rate constants and with respects to initial concentrations. For a variable X of the model and a parameter p, the scaled steady state sensitivity coefficient of X with respect to p is $\lim_{t\to\infty} \partial \ln(X)/\partial \ln(p)(t)$. These coefficients measure the relative change in steady state when some parameter is changed with an infinitesimally small amount. They help identify the most important steps in the heat shock response network. A first observation was that the sensitivity coefficients of all variables of the model with respect to reaction rate constants k_1^-, k_2^-, k_3^-, and k_7 are negligible. This suggested that the respective reactions may have negligible effect on the overall behavior of the model. To test this prediction, we removed reaction (7) and the right-to-left directions of reactions (1), (2) and (3). The reactions of the reduced model are in Table 4 and their kinetic constants are unchanged with respect to the basic model. It turned out that the reduced model performs equally well as the basic model in all validation tests described above. Our model thus predicted that hsf dimers and trimers are very stable and do not break spontaneously at a significant rate. The spontaneous unbinding of an hsf trimer from hse (without the involvement of hsp) was also insignificant. Interestingly, while reaction (7) (hsp breaking hsf trimers) did not have a significant role and could be eliminated from the model, reaction (6) (hsp breaking hsf dimers) did have a significant influence on several variables of the model, including hsp and mfp.

We focused on the sensitivity coefficients of hsp and mfp, the main drivers of the response. They showed a direct correlation between variations in the steady state levels of hsp and mfp, not surprising given the chaperoning role of hsp.

Table 4: **The list of reactions in the reduced molecular model. Reactions** (1) **(right-to-left),** (2)**(right-to-left),** (3)**(right-to-left), and** (7) **were eliminated from the basic model in Table 1 without affecting its numerical behavior.**

Reaction
$2\,\mathsf{hsf} \rightarrow \mathsf{hsf}_2$
$\mathsf{hsf} + \mathsf{hsf}_2 \rightarrow \mathsf{hsf}_3$
$\mathsf{hsf}_3 + \mathsf{hse} \rightarrow \mathsf{hsf}_3\colon \mathsf{hse}$
$\mathsf{hsf}_3\colon \mathsf{hse} \rightarrow \mathsf{hsf}_3\colon \mathsf{hse} + \mathsf{hsp}$
$\mathsf{hsp} + \mathsf{hsf} \leftrightarrow \mathsf{hsp}\colon \mathsf{hsf}$
$\mathsf{hsp} + \mathsf{hsf}_2 \rightarrow \mathsf{hsp}\colon \mathsf{hsf} + \mathsf{hsf}$
$\mathsf{hsp} + \mathsf{hsf}_3\colon \mathsf{hse} \rightarrow \mathsf{hsp}\colon \mathsf{hsf} + \mathsf{hse} + 2\,\mathsf{hsf}$
$\mathsf{hsp} \rightarrow$
$\mathsf{prot} \rightarrow \mathsf{mfp}$
$\mathsf{hsp} + \mathsf{mfp} \leftrightarrow \mathsf{hsp}\colon \mathsf{mfp}$
$\mathsf{hsp}\colon \mathsf{mfp} \rightarrow \mathsf{hsp} + \mathsf{prot}$

Their largest sensitivity coefficients are in Table 5 and can be interpreted as follows. The coefficients with respect to k_5^+ and k_5^- being the largest identified reaction (5) in Table 1 as the most important feedback loop in our model. In one direction of reaction (5), hsf is sequestrated, leading eventually to a suppression of the transcription, in concert with reaction (8), and consequently, to a reduction in hsp and an increase in mfp. In the other direction of reaction (5), hsp and hsf levels are increased, both leading to increasing hsp and decreasing mfp. The next largest coefficients are with respect to k_1^+, k_2^+ and k_4: reactions (1), (2), and (4) all contribute to increasing the level of transcription and by consequence, the level of hsp as follows: hsf dimers or trimers form at a higher rate, or hsf_3 binds to hse at a higher rate. Reactions (6), (8) and (9) (see the sensitivity coefficients with respect to k_6, k_8, k_9) have a countering effect on the level of transcription or directly on that of hsp: hsf: dimers are dissipated at a higher rate and are less able to form trimers, hsf_3 unbinds from hse at a higher rate, or hsp degrades at a higher rate. The only reactions that influenced the level of mfp but not that of hsp are (11) and (12), see the sensitivity coefficients with respect to k_{11}^+, k_{11}^-, and k_{12} in Table 5. These reactions control the chaperoning and the refolding of mfp, while not consuming hsp.

The most significant sensitivity coefficient of hsp and of mfp with respect to initial concentrations was that depending on $\mathsf{hsp}\colon \mathsf{hsf}(0)$, where $\mathsf{hsp}\colon \mathsf{hsf}(0)$ denotes the initial level of hsp: hsf, with similar notations for the other variables of the model. On the other hand, the sensitivity coefficients of both hsp and of mfp on the other forms of hsf (monomer, dimer, trimer) were negligible. This is a direct consequence of the fact that almost all initial amount of hsf is sequestered by hsp, while the initial levels of dimers and trimers are very low (in line with

Table 5: **The largest scaled steady state sensitivity coefficients of hsp and mfp. The coefficients are identical at $37°C$ and $42°C$.**

Description	p	Sensitivity $\frac{\partial \ln(\mathsf{hsp})}{\partial \ln(p)}\|_{t\to\infty}$	Sensitivity $\frac{\partial \ln(\mathsf{mfp})}{\partial \ln(p)}\|_{t\to\infty}$
Sequestration of hsf by hsp	k_5^+	-0.50	0.50
Dissipation of hsp: hsf	k_5^-	0.50	-0.50
Formation of hsf dimers	k_1^+	0.17	-0.17
Formation of hsf trimers	k_2^+	0.17	-0.17
Transcription, translation	k_4	0.17	-0.17
Affinity of hsp for hsf_2	k_6	-0.17	0.17
Affinity of hsp for hsf_3: hse	k_8	-0.17	0.17
Degradation of hsp	k_9	-0.17	0.17
Affinity of hsp for mfp	k_{11}^+	0.00	-1.00
Dissipation of hsp: mfp	k_{11}^-	0.00	0.24
Refolding	k_{12}	0.00	-0.24
Initial level of hsp: hsf	hsp: hsf(0)	0.50	-0.50

experimental observations of [7]). As such the dependency on hsp: hsf(0) should rather be interpreted as a dependency on the total initial amount of hsf. This interpretation was supported by the following numerical experiment. We set hsp: hsf(0) to 0 and increase correspondingly hsp(0) and hsf(0) (or, alternatively, $\mathsf{hsf}_2(0)$, or $\mathsf{hsf}_3(0)$) in such a way that the initial total amount of hsp and of hsf is unchanged. Then hsp and mfp got significant sensitivity coefficients with respect to hsf(0) ($\mathsf{hsf}_2(0)$, or $\mathsf{hsf}_3(0)$, respectively) and negligible with respect to hsp: hsf(0). Distributing the initial amount of hsf among its various forms had however a crucial effect on the speed and on the peak of the response.

The scaled steady state sensitivity coefficients of both hsp and mfp with respect to hse(0) were negligible. This result is explained by the fact that we considered the sensitivities around the steady state. For example, with fewer hse(0), the response will eventually be able to approach the same steady state, albeit the transcription stays at the 100% level for a longer time (because a lower [hse] becomes a bottleneck of the response). Interestingly, with a higher hse(0), the time evolution of the response remained unchanged, indicating that as long as hse(0) was higher than a certain threshold, its numerical value was irrelevant for the model prediction. This was indeed confirmed by numerical simulations.

The sensitivities of both hsp and mfp (and in fact those of all variables) with respect to hsp(0) were also negligible. The reason for this is that the system was able to self-regulate a lower/higher hsp(0) and eventually approach the same steady state. On the other hand, a lower/higher hsp(0) did have an impact on the time evolution of the response.

Alternative numerical model fits The reaction rate constant values of our mathematical model were obtained by performing parameter estimation with

respect to the experimental data of [6]. We address in this section the question of the uniqueness of the set of parameters that fulfill the imposed conditions, a problem that is also known as the *model identifiability*. By repeating from scratch the whole parameter estimation procedure, we obtained several different sets of parameter values that result both in a good fit of the model to the experimental data, as well as in initial values that are steady-states of the model at 37 °C. It turned out however that all these parameter sets failed the model validation tests discussed above with respect to the qualitative observations concerning the behavior of cells under stress. This does not prove that our heat shock response model is uniquely identifiable. However, it does suggest that fitting the model to the experimental data in [6] and to the steady-state condition for the initial values is a difficult numerical problem.

A thorough method of searching for alternative numerical model fits is to perform a systematic parameter scan in the space determined by the considered ranges of parameter values. This means that for each parameter, one partitions its value range into a large number of subintervals (say, tens of thousands of them) and samples values for the parameter from all of them. One then tests the quality of the model fit for all possible combinations of parameter samples to yield a thorough sampling of the model behavior throughout the multi-dimensional parameter space. Unfortunately, the direct implementation of this idea is intractable for models with more than a few parameters due to the combinatorial explosion of the number of simulations that need to be run. A fast, practical solution to this problem is to apply the *Latin Hypercube Sampling* method (LHS), first introduced in [34]. This method provides samples which are uniformly distributed over each parameter while the number of samples is independent of the number of parameters, see also [35–37] for applications of this method. We describe the sampling scheme briefly in the following, in the simpler case when the parameter values are uniformly distributed in their range interval. One first chooses the desired size N of the sampling set. The range interval of each parameter is then partitioned into N non-overlapping intervals of equal length. For each parameter, we randomly select N numerical values, one from from each interval of the partition. We collect the N sampled values for the i-th parameter of the model on the i-th column of a $N \times p$ matrix, where p is the number of parameters. One then randomly shuffles the values on each column. The result of the procedure is read from the rows of the matrix: each of the N rows of the matrix contains numerical values for each of the p parameters. For a detailed description of this sampling scheme we refer to [34].

Based on the LHS method we have implemented the following strategy to look for alternative models fits that are in agreement with the experimental data of [6], and satisfy the steady-state condition for the initial values. First, by applying the LHS method, we sampled $N = 100.000$ sets of parameter values. For each set, we estimated numerically the steady state of the model for a temperature value of 37 °C. We then set the initial state of the model as the calculated steady state. We simulated the model for 14400 seconds at a temperature of 42 °C. Finally, we classified as *non-responsive* those parameter samples that led to low DNA binding level at the peak of the response, and excluded them from further analysis. We obtained that only 31.506 out of the 100.000 samples were responsive, already a result pointing to difficulties in finding satisfactory alternative numerical fits. We analyzed each of these models as follows. For each model, we made a scatter plot for each variable and each parameter where

we plotted the steady state values of each variable at 37 °C, against the values of the parameter. We discuss here only a few of the plots. All plots are available as supplementary materials at [38].

We compared the obtained results with the steady state values of our basic model (called also reference model in the following) at 37 °C. As can be seen in Figure 3a, only very few of the sampled models were capable of reaching low levels of DNA binding at the steady state. This showed that most of the alternative fits predicted high levels of gene transcription in the absence of the heat shock, a contradiction of the available biological evidence, see [7]. In the case of hsf, none of the sampled models reached such a low level as the reference model, see Figure 3b. Moreover, the reference model is one of the very few models in which most of the hsf molecules are sequestered by hsp, see Figure 3c. This indicates that at the temperature of 37 °C the response mechanism is turned off, which is in excellent agreement with biological observations, see [7]. These outcomes are also supported by the results obtained for hsf dimers presented in Figure 3d, where the basic model reaches the lowest values. This is also in agreement with the observation that hsf dimers are unnoticeable in biological experiments.

We also compared the predictions of all the sampled models at 42 °C with respect to the experimental data of [6]. The same score function which was used in the case of parameter estimation, i.e. the sum of of squares of the residues, was computed for all considered models. The results are depicted in the form of a scatter plot and its zoomed in version in Figure 4a and Figure 4b, respectively. Our reference model obtained the lowest score of around 12, while the 13 best fits of the sampled models were in the range between 300 and 1000. All the other models had much worse scores, of more than 1000.

While it is likely that a model of this size is not uniquely identifiable, our parameter scan showed that finding parameter values satisfying our model constraints is far from being easy. This is evident both from the plots of the model deviation from the experimental data under stress (as measured by the score function, Figure 4a and Figure 4b) as well as from the plots of the model behavior in the absence of stress (Figure 3a–3d). Even more, about two thirds of the parameter samples led to none-responsive models, i.e., models that yield an insufficient response under stress.

Discussion

We presented a simple molecular model for the heat shock response, based on standard molecular biology only. The mathematical model was validated based both on existing data from the literature, as well as on our novel experimental evidence. The numerical simulations of the model correlate well with predictions reported elsewhere in the literature.

Using sensitivity coefficients we predict that a number of reactions have a negligible effect on the model and could be removed without affecting its numerical behavior. We also identify the reactions with the most significant effect on hsp and on mfp. This is a useful, still not fully exploited potential of mathematical modeling in biology. We have started from a molecular model that incorporated a number of reactions that could in principle take place even though no direct experimental evidence in their support exists: the dissipation

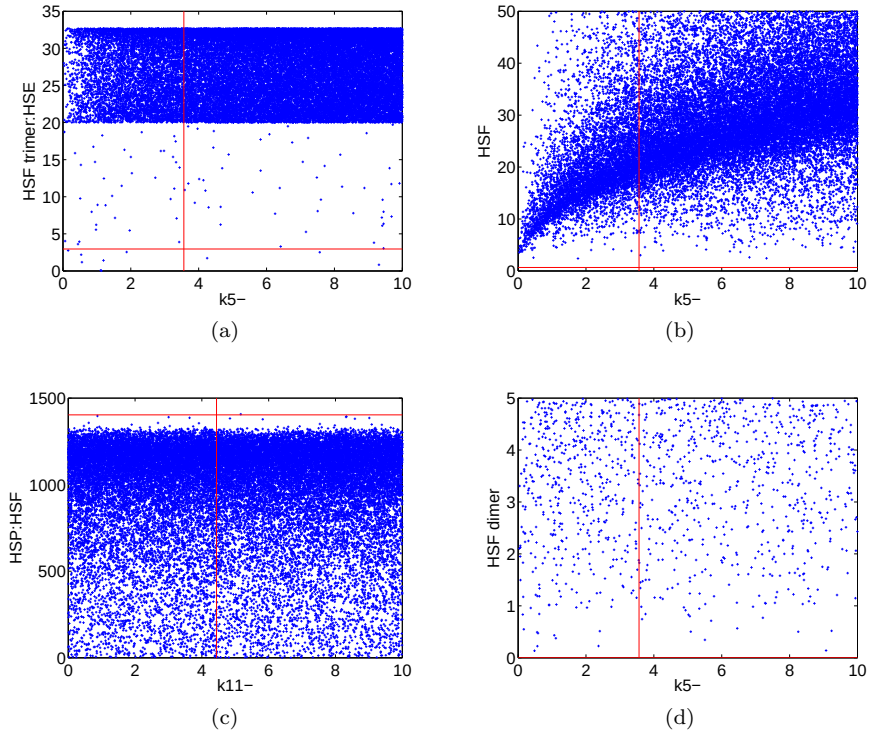

Figure 3: Scatter plots of the steady state values at 37 °C of the sampled models (blue crosses) and the basic model (red horizontal line). The red vertical line indicates the parameter value of the basic model. The plots of hsf (b) and hsf_2 (d) are zoomed in, hence not all points are present, i.e. the values of the remaining steady states were higher than the maximum value on the y-axes.

of dimers and of trimers, or the spontaneous unbinding of hsf_3 from hse. The mathematical analysis of the model points out to the fact that these reactions have a negligible effect on the overall behavior of the model and it suggests that they could be eliminated from the model. These results help simplify the molecular model which in turn is important for further, more complex analysis of the associated mathematical model and for their integration into larger models. They can also be regarded as predictions that could be used in further validation experiments. It is important to recognize however that these results are dependent on the numerical values of the reaction rate constants and those of the initial concentrations. Different numerical values for these parameters may lead to different results. This is a general problem of any mathematical modeling project, see [33] for a discussion on the computational difficulties of this task. Clearly, having the model validated in a number of experimental setups helps increase the confidence in the numerical values we report.

Related models Several mathematical models for the heat shock response, both for prokaryotes and for eukaryotes have been proposed in [12, 25–29]. We compare in here our model with the ones in [12] and [25] that seem most related

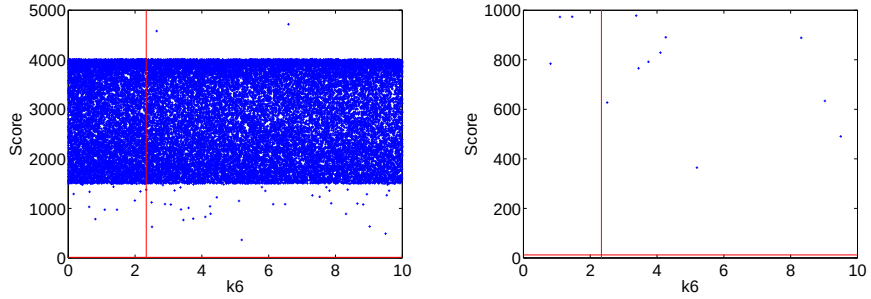

(a) (b)

Figure 4: Scatter plot (a) and its zoomed in version (b) of the score measuring the fit of the sampled models (blue crosses) and the basic model (red horizontal line) with respect to the experimental data. The red vertical line indicates the parameter value of the basic model.

to ours.

The model in [12] considers, as we do, hsf and its dimerization and trimerization, heat-induced misfolding, but it also considers other components: mRNA molecules and nascent proteins chains, including their interactions with HSP. The model was tested against experimental data obtained from Reuber H35 rat hepatoma cells on the synthesis of the hsp70 family members. One of the shortcomings of the model in [12] is that it does not consider the details of the hsp-regulated transcription. Instead the control is realized in the model through hsp-blocking of mRNA and through hsp: hsf bindings. Another concern has to do with the treatment of mRNA: it is not produced as a result of DNA transcription and it is not used directly in a model for protein synthesis, the crucial feedback regulatory motif in our model. Instead, mRNA is used in a hypothetical reaction of binding to misfolded proteins. Such a reaction leaves only part of mRNA molecules as "healthy" and their proportion is then used to model the slowing reaction rate of hsp binding to nascent protein chains. (Many of these steps lack experimental support.) The same effect can however be obtained, as suggested in our model, based on the observation that hsp molecules are competed on, according to the mass-action principle, both by misfolded proteins (present on a massive scale under stress), and by nascent proteins chains.

The model in [25] examines the eukaryotic heat shock response based on hsp, hsf and hse, as we have, but also includes hsp mRNA molecules, a stimulus signal, and a stress kinase. The hsp synthesis is controlled through hsp-regulated DNA transcription, through hsp: hsf binding, but also through the fact that the stability of hsp mRNA molecules is increased due to stress. Moreover, the model considers the activation of hsf molecules when bounded to hse, mediated by the stress kinase. In turn, the stress kinase is activated by the stimulus signal. On the other hand, dimerization and trimerization of hsf molecules is not considered, and neither is the degradation of hsp. The model is tested against experimental data from HeLa cells [6]. The main difference with respect to our model is the fact that the heat shock is modeled in an abstract way through the stimulus signal and the stress kinase, rather than mechanistically

through mfp as the initiating signal, as we do.

A recent paper, [28], takes a completely different modeling approach. Starting from available experimental data on the response of Chinese hamster ovary cells to heat shock, rather than a set of reactions, they develop a stochastic theoretical model accounting for the observed mean response. Interestingly, they rediscover in this way the hsf-regulated transactivation of hsp-encoding genes.

In another recent paper, [29], the molecular model (summarized from [21]) includes several of the reactions in our model. Importantly, they do not consider the heat-induced protein misfolding. Also, in the associated mathematical model, only a part of the molecular model is analyzed.

A molecular model that is similar to the one we consider in this paper has been recently presented in [39]. Some of the molecular details of the model in [39] are however different and in fact, their model includes reactions (such as the concomitant binding of three different molecules) whose kinetics are highly unfavorable. The major differences however are in the numerical evaluations of the model. While the authors of [39] have an ad-hoc choice of parameter values, the bulk of our work is in extensive parameter estimation and numerical validation of the model, based both on literature data, as well as on novel experiments.

Extensions The current model can be extended to include several other aspects of the heat shock response. For example, one may include in the model the heat-induced misfolding and chaperon-assisted refolding of both hsp and hsf. Indeed, since both hsp and hsf are proteins, they are exposed to heat-induced misfolding. This extension includes in the model a most attractive feature of living cells: the repair mechanism is subject to failure, but it has capabilities to repair itself. In terms of the molecular model, the model extension consists of adding 6 reactions:

Misfolding:	$\mathsf{hsp} \to \mathsf{mhsp}$
	$\mathsf{hsf} \to \mathsf{mhsf}$
Sequestration:	$\mathsf{hsp} + \mathsf{mhsp} \leftrightarrow \mathsf{hsp{:}\,mhsp}$
	$\mathsf{hsp} + \mathsf{mhsf} \leftrightarrow \mathsf{hsp{:}\,mhsf}$
Refolding:	$\mathsf{hsp{:}\,mhsp} \to 2\,\mathsf{hsp}$
	$\mathsf{hsp{:}\,mhsf} \to \mathsf{hsp} + \mathsf{hsf}$

One way to include this model extension in the mathematical model is to assign each reaction a new kinetic parameter and measure or estimate their numerical values in such a way that the fit and the model validation with respect to experimental data remain excellent. Another way, that we adopted, is to assume a principle of uniform biochemistry: every two similar reactions in the model should be driven by the same kinetic constants. We observe that each of the reactions in the model extension above has a correspondent in the basic model: the misfolding reactions are similar to reaction (10), the sequestration reactions are similar to (11) and the refolding reactions are similar to (12). Therefore, we can use for the model extension similar kinetics as in the basic model: ϕ_T as reaction rate coefficient for the misfolding reactions, k_{11}^+, k_{11}^- for the sequestration reactions, and k_{12} for the refolding reactions (with the same numerical values as for the basic model). Remarkably, the fit and the validation of the extended model remains essentially unchanged. For details we refer to [31].

Including the phosphorylation of hsf and its role on the hsf activity is attractive, but it appears to be very challenging. The difficulty is in distinguishing all phosphorylation states of all known phosphorylation sites (currently at least 14 of them, see [3, 7]) of hsf. This leads to an exponential increase in the number of variables in our model. To start with, we have considered only one phosphorylation site for each hsf. We also asked in the extended model that an hsf trimer is only able to promote gene transcription if it has at least two of its three sites phosphorylated. The extended model includes all possible phosphorylation states of hsf, hsf_2, hsf_3, hsp: hsf, as well as protein kinases and phosphatases (which may be misfolded/refolded). The new model consists of 61 reactions and 26 reactants (I.Petre et al, unpublished data).We succeeded fitting the model to the data on DNA binding from [6] in such a way that the rate constants of the reactions of the basic model remain unchanged. When considering also the phosphorylation data of [6], the combined fit was very poor. This may indicate that the rate constants of the basic model should be re-estimated in this case, leading to a very challenging computational task. This difficulty points also to an intrinsic problem of modeling with differential equations: they are describing explicitly all variables in the model, even when many of them are essentially just duplicates of each other. A novel mathematical modeling methodology able to describe models in terms of various independent components and the communication between them (such as done in concurrency in Computer Science), may be more suitable in such setups.

Parameter scanning as a local optimization method A major difficulty we have encountered when performing parameter estimation was to fit the time-dependent behavior of the model with respect to experimental data, while making sure that the initial values are an approximation of a steady state of the model. Indeed, the steady state of the model is a function of the parameters (and of other variables, such as total mass of various species). Once a good fit with respect to experimental data was found, our approach was to replace the initial values with the steady state of the obtained model at 37 °C and hope that the model fit at 42 °C is not destroyed. This is the main reason why parameter estimation was the most time-consuming part of the work.

The parameter scanning method that we have used when analyzing our model could in fact be used as a local optimization method that takes into consideration simultaneously the steady state condition and the stress-induced response of the model. The idea is that for a model that is continuous in all of the parameters (as ours is), the procedure identifies a region in the multi-dimensional parameter space where a local minimum of the score function is found. Iterating this procedure yields a realization of a local minimum of the score function, while the initial state of the model is a steady state for a temperature of 37 °C.

Applicability Mathematical modeling of biological processes may allow reasoning about uncertain or incomplete subparts of the process. For example, when constructing our molecular model, see Table 1, all reactions were considered reversible, unless they were definitely known to be unidirectional. E.g., we decided to include also reaction $\mathsf{hsf}_3 \rightarrow \mathsf{hsf} + \mathsf{hsf}_2$, although arguments based on the stability of trimers and the transient nature of dimers could be used

against it. The corresponding mathematical model and its fitting help handle such incomplete information. It turns out that our model fit gives a very low rate constant for that reaction, suggesting that the reaction could be omitted altogether from the model. Arguments based on sensitivity analysis help identify more reactions that can be eliminated from the model without affecting its time evolution.

The heat shock response was amongst the primordial gene networks given the fluctuating environment and the necessity to establish proteostasis networks. The minimal mathematical model we proposed in this paper, based on stress-induced activation and feedback regulation only, may be useful also for the understanding of other forms of stress signalling or gene expression. The numerical techniques that we have used in this paper for identifying the essential components of the regulatory network may also be applicable in other mathematical modeling projects.

Materials and methods

Construct information. To make the hsp70promoter700-yfp construct, the CMV promoter was removed from pEYFP-N1 (Clontech) by inserting an XhoI site before the start of the CMV promoter by site directed mutagenesis using the primer 5'-TCTGTGGATAAGATCTCGAGCGCCATGCAT-3' and its complement. The CMV promoter was deleted by digesting with XhoI, which cleave the new plasmid both in front of the CMV sequence and after this sequence in the MCS. The cleaved fragments were separated by electrophoresis, and the 4.1 kb fragment lacking the CMV promoter sequence was isolated and ligated to form pEYFPΔCMV. To add the hsp70 promoter in front of yfp, the 712 bp fragment of the hsp70 promoter was digested from pGL-712-hsp70 (a kind gift from A. Stanhill and D. Engelberg, Jerusalem, Israel) using XhoI and HindIII, and subcloned into the pEYFPΔCMV plasmid.

Cell culture and heat shock experiments. K562 cells were maintained in RPMI-1640 medium supplemented with 10% fetal calf serum, 2 mM L-glutamine, penicillin and streptomycin at $37°C$ in a 5% CO2 humidified atmosphere. 5.0×10^6 K562 cells were transfected with hsp70promoter700-yfp plasmid by electroporation (250V per 975 μF; GenePulser II electroporator, BioRad laboratories). hsp70promoter700-yfp stable cell pools were selected with geneticin. For heat shock treatments, 0.5×10^6 ml^{-1} hsp70promoter700-yfp stably expressing K562 cells were transferred to RPMI-1640 medium with supplements pre-warmed to $42°C$. Heat shock was induced at $42°C$ in a 5% CO2 humidified atmosphere for the following time points prior to sampling: 36hr, 33hr, 30hr, 27hr, 24hr, 21hr, 18hr, 12hr, 10hr, 8hr, 6hr, 4hr, 2hr, 1hr and 0hr (control). Cells were allowed to recover post-heat shock for 2hrs at $37°C$. Fluorescence intensity of yfp was measured by flow cytometry with FACScan (Becton Dickinson). Samples from heat-shocked cells were lysed and separated by SDS-PAGE and analyzed by western bloting.

Acknowledgments

This work has been partially supported by the following grants from Academy of Finland: project 108421 (IP), project 203667 (A.Mizera), the Center of Excellence on Formal Methods in Programming (R-J.B.).

References

[1] Powers MV, Workman P (2007) Inhibitors of the heat shock response: Biology and pharmacology. *FEBS Lett.* **581**(19): 3758–3769

[2] Chen Y, Voegli TS, Liu PP, Noble EG, Currie RW (2007) Heat shock paradox and a new role of heat shock proteins and their receptors as anti-inflammation targets. *Inflamm Allergy Drug Targets* **6**(2): 91–100

[3] Voellmy R, Boellmann F (2007) Chaperone regulation of the heat shock protein response. *Adv Exp Med Biol* **594**: 89–99

[4] Balch WE, Morimoto RI, , Dillin A, Kelly JW (2008) Adapting proteostasis for disease intervention. *Science* **319**, 916–919

[5] Morimoto RI (2008) Proteotoxic stress and inducible chaperone networks in neurodegenerative disease and aging. *Genes Dev* **22**: 1427–1438

[6] Kline MP, Morimoto RI (1997) Repression of the heat shock factor 1 transcriptional activation domain is modulated by constitutive phosphorylation *Molecular and Cellular Biology* **17**(4): 2107–2115

[7] Holmberg CI, Tran SE, Eriksson JE, Sistonen L (2002) Multisite phosphorylation provides sophisticated regulation of transcription factors. *Trends Biochem Sci* **27**(12): 619–627

[8] Voellmy R (1994) Transduction of the stress signal and mechanisms of transcriptional regulation of heat shock/stress protein gene expression in higher eukaryotes. *Crit Rev Eukaryot Gene Expr* **4**: 357–401

[9] Morimoto RI, Jurivich DA, Kroger PE, Mathur SK, Murphy SP, et al (1994) Regulation of heat shock gene transcription by a family of heat shock factors. In: Morimoto RI, Tissières A, Georgopoulos C (eds.) *The biology of the heat shock proteins and molecular chaperones*: 417–455

[10] Abravaya K, Myers M, Murphy S, Morimoto RI (1992) Human Heat Shock Protein HSP70 Interacts with HSF, the Transcription Factor That Regulates Heat Shock Gene Expression. *Genes Dev* **6**: 1153–1164

[11] Shi Y, Mosser D, Morimoto RI (1998) Molecular Chaperones as HSF1 Specific Transcriptional Repressors. *Genes Dev* **12**: 654–666

[12] Peper A, Grimbergen CA, Spaan JAE, Souren JEM, van Wijk R (1997) A mathematical model of the hsp70 regulation in the cell. *Int. J. Hyperthermia* **14**(1): 97–124

[13] Lepock JR, Frey HE, Ritchie KP (1993) Protein denaturation in intact hepatocytes and isolated cellular organelles during heat shock. *The Journal of Cell Biology* **122**(6): 1267–1276

[14] Guldberg CM, Waage P (1864) Studies Concerning Affinity. *C. M. Forhandlinger: Videnskabs-Selskabet i Christiana* **35**

[15] Guldberg CM, Waage P (1879) Concerning Chemical Affinity. *Erdmann's Journal fr Practische Chemie* **127**: 69–114.

[16] Hoops S, Sahle S, Gauges R, Lee C, Pahle J, Simus N, Singhal M, Xu L, Mendes P, Kummer U (2006) COPASI a COmplex PAthway SImulator. *Bioinformatics* **22**: 3067–3074

[17] Jones CM et al , Henry ER, Hu Y, Chan C, Luck SD, Bhuyan A, Roder H, Hofrichter J, Eaton WA (1993) Fast events in protein folding initiated by nanosecond laser photolysis. *Proc. Natl. Acad. Sci. USA* **90**: 11860-64

[18] Ballew RM, Sabelko J, Gruebele M (1996) Direct observation of fast protein folding: the initial collapse of apomyoglobin. *Proc. Natl. Acad. Sci. USA* **93**: 5759-64

[19] Donati YRA, Slosman DO, Polla BS (1990) Oxidative injury and the heat shock response. *Biochem Pharmacol* **40**: 2571–2577

[20] Pockley AG (2003) Heat shock proteins as regulators of the immune response. *The Lancet* **362**(9382): 469–476

[21] Morimoto RI (1998) Regulation of the heat shock transcriptional response: cross talk between a family of heat shock factors, molecular chaperones, and negative regulators. *Genes Develop* **12**: 3788–3796

[22] Parsell DA, Lindquist S (1993) The function of heat-shock proteins in stress tolerance: degradation and reactivation of damaged proteins. *Ann Rev Genetics* **27**: 437–496

[23] Ciocca DR, Calderwood SK (2005) Heat shock proteins in cancer: diagnostic, prognostic, predictive, and treatment implications. *Cell stress and chaperones* **10**(2): 86–103

[24] Vastag B (2006) HSP-90 inhibitors promise to complement cancer therapies. *Nature Biotechnology* **24**(11): 1307

[25] Rieger TR, Morimoto RI, Hatzimanikatis V (2005) Mathematical Modeling of the Eukaryotic Heat Shock Response: Dynamics of the Hsp70 Promoter. *Biophysical Journal* **88**: 1646–1658

[26] El Samad H, Kurata H, Doyle JC, Gross CA, Khammash M (2005) Surviving heat shock: Control strategies for robustness and performance. *Proc Natl Acad Sci* **102**(8): 2736–2741

[27] Srivastava R, Peterson MS, Bentley WE (2001) Stochastic kinetic analysis of the Escherichia coli stress circuit using $\sigma^3$2-trageted antisense. *Biotechnol Bioeng* **75**(1): 120–129

[28] Lipan O, Navenot J-M, Wang Z, Huang L, Peiper SC (2007) Heat Shock Response in CHO Mammalian Cells Is Controlled by a Nonlinear Stochastic Process. *PLoS Computational Biology* **3**(10): 1859–1870

[29] Remondini D, Bernardini C, Forni M, Bersani F, Castellani GC, Bacci ML (2006) Induced Metastable Memory in Heat Shock Response. *J. Biol. Physics* **32**: 49–59

[30] Abravaya K, Philips B, Morimoto RI (1991) Attenuation of the heat-shock response in Hela-cells is mediated by the release of bound heat-shock transcription factor and is modulated by changes in growth and in heat-shock temperatures *Genes Dev* **5**(11): 2117–2127

[31] Petre I, Mizera A, Hyder CL, Mikhailov A, Eriksson JE, Sistonen L, Back R-J (2009) A new mathematical model for the heat shock response. In: Condon A, Harel D, Kok J, Salomaa A (Eds.) *Algorithmic bioprocesses*, Springer, 411–428

[32] Turanyi T (1990) Sensitivity analysis of complex kinetic systems – tools and applications *J. Math Chem.* **5**(3): 203–248

[33] Chen WW, Schorberl B, Jasper PJ, Niepel M, Nielsen UB,Lauffenburger DA, Sorger PK (2009) Input-output behavior of ErbB signaling pathways as revealed by a mass action model trained against dynamic data *Molecular Systems Biology* **5**: 1–19

[34] McKay MD, Beckman RJ, Conover WJ (1979) *Technometrics* **21**(2), 239-245

[35] Helton JC, Davis FJ (2002) Illustration of Sampling-Based Methods for Uncertainty and Sensitivity Analysis. Risk Analysis **22**(3): 591–622

[36] Helton JC, Davis FJ (2003) Latin hypercube sampling and the propagation of uncertainty in analyses of complex systems. Reliability Engineering and System Safety **81**: 23–69

[37] Oberguggenberger M, King J, Schmelzer B (2009) Classical and imprecise probability methods for sensitivity analysis in engineering: A case study. Int J Approx Reasoning **50**: 680-693

[38] http://combio.abo.fi/hsr/plots.zip

[39] Szymańska Z, Zylicz M (2009) Mathematical modeling of heat shock protein synthesis in response to temperature change. J Theoret Biol **259**: 562–569